



Role of Myocardial Extracellular Volume Fraction Measured with Magnetic Resonance Imaging in the Prediction of Left Ventricular Functional Outcome after Revascularization of Chronic Total Occlusion of Coronary Arteries

Yinyin Chen, PhD¹, Xinde Zheng, MB¹, Hang Jin, MD, PhD¹, Shengming Deng, PhD², Daoyuan Ren, MD³, Andreas Greiser, MD, PhD⁴, Caixia Fu, MD⁵, Hongxiang Gao, MD⁶, Mengsu Zeng, MD, PhD¹

¹Department of Radiology, Zhongshan Hospital, Fudan University; Department of Medical Imaging, Shanghai Medical School, Fudan University and Shanghai Institute of Medical Imaging, Shanghai, China; ²Department of Nuclear Medicine, The First Affiliated Hospital of Soochow University, Suzhou, China; ³Department of Cardiology, Zhongshan Hospital, Fudan University, Shanghai, China; ⁴Siemens Healthcare GmbH, Erlangen, Germany; ⁵Siemens Shenzhen Magnetic Resonance (C.F.), Shenzhen, China; ⁶Department of Clinical Laboratory, Zhongshan Hospital, Fudan University, Shanghai, China

Objective: The purpose of this study was to prospectively investigate the value of the myocardial extracellular volume fraction (ECV) in predicting myocardial functional outcome after revascularization of coronary chronic total occlusion (CTO).

Materials and Methods: Thirty patients with CTO underwent cardiovascular magnetic resonance (CMR) before and 6 months after revascularization. Three baseline markers of functional outcome were evaluated in the dysfunctional segments assigned to the CTO vessels: ECV, transmural extent of infarction (TEI), and unenhanced rim thickness (RIM). At the global level, the ECV values of the whole myocardium with and without a hyperenhanced region (global and remote ECV) were respectively measured.

Results: In per-segment analysis, ECV was superior to TEI and RIM in predicting functional recovery (area under receiver operating characteristic curve [AUC]: 0.86 vs. 0.75 and 0.73, all p values < 0.010), and it emerged as the only independent predictor of regional functional outcome (odds ratio [OR] = 0.83, 95% confidence interval [CI]: 0.77–0.89; p < 0.001) independent of collateral circulation. In per-patient analysis, global baseline ECV was indicative of ejection fraction (EF) at the follow-up examination (β = -0.61, p < 0.001) and changes in EF (β = -0.57, p = 0.001) in multivariate regression analysis. A patient with global baseline ECV less than 30.0% (AUC, 0.93; sensitivity 94%, specificity 80%) was more likely to demonstrate significant EF improvement (OR: 0.38; 95% CI: 0.17–0.85; p = 0.019).

Conclusion: Extracellular volume fraction obtained by CMR may provide incremental value for the prediction of functional recovery both at the segmental and global levels in CTO patients, and may facilitate the identification of patients who can benefit from revascularization.

Keywords: *Magnetic resonance imaging; Cardiac; T1 mapping; Extracellular volume fraction; Chronic total occlusion; Coronary arteries; Myocardial infarction; Myocardial ischemia; Late gadolinium enhancement*

Received January 26, 2018; accepted after revision June 11, 2018.

This study was supported by the National Natural Science Foundation of China (Grant No.: 81701643 and 81601522) and Zhongshan Hospital Fudan University Science Foundation for youth (Grant No.: 2017ZSQN24).

Corresponding author: Mengsu Zeng, MD, PhD, Department of Radiology, Zhongshan Hospital, Fudan University, No. 180 Fenglin Road, Shanghai 200032, China.

• Tel: (86) 64041990-2130 • Fax: (86) 64439906 • E-mail: zengmengsu@outlook.com

This is an Open Access article distributed under the terms of the Creative Commons Attribution Non-Commercial License (<https://creativecommons.org/licenses/by-nc/4.0>) which permits unrestricted non-commercial use, distribution, and reproduction in any medium, provided the original work is properly cited.

INTRODUCTION

Coronary chronic total occlusion (CTO) is defined as a complete occlusion confirmed by coronary angiography over a period of 3 months, and its prevalence has been reported as being 20–30% (1, 2). Successful CTO percutaneous coronary intervention (PCI) leads to angina relief, lower mortality, as well as improvement of left ventricular (LV) function (3-5). In the setting of CTO with chronic myocardial ischemia, the affected myocardium shows depressed contractility to compensate the insult, while the collateral circulation improves blood supply to areas of downstream myocardium, and is closely associated with regional wall motion (6, 7). However, whether the collateral circulation plays a role in the prediction of functional recovery in CTO patients has not been studied.

Late gadolinium-enhanced cardiovascular magnetic resonance (CMR) is widely used to predict the likelihood of functional recovery after revascularization. Most studies use a cutoff value of less than 50% transmural extent of infarction (TEI) to identify recovery of regional function, and this technique has an overall accuracy of 70% (8). Unenhanced rim thickness (RIM) is the thickness of the epicardial myocardial area without late gadolinium enhancement (LGE), and serves as a baseline marker for predicting functional recovery, with the reported threshold ranging from 3.0 mm to 4.5 mm (9, 10).

More recent studies have shown that the extracellular volume fraction (ECV) can be non-invasively measured based on native and post-contrast T1 mapping and reflects the size of the extracellular space. ECV quantification has been confirmed to be a robust tool for the identification of the extent of myocardial injury or degeneration in a variety of cardiac diseases (11-13). Previous studies reported that the degree of degenerative changes in the dysfunctional myocardium determines the likelihood of recovery after revascularization (10), and the epicardial unenhanced rim showed greater relevance as a predictor of functional recovery (14). A greater degree of degenerative changes, manifested by replacement of cardiomyocytes by fibrosis, leads to the increased extracellular space (10), thereby increasing ECV. Based on these insights, the purpose of this study was to investigate the additional value of ECV derived from T1 mapping for prediction of functional recovery in comparison with standard CMR measurement. The second goal was to demonstrate the influence of collateral circulation on the functional recovery in CTO territories.

MATERIALS AND METHODS

Patient Population

Our Institutional Review Board committee approved the study; all patients provided written informed consent. Between September 2013 and August 2015, patients with angiographically confirmed CTO scheduled for interventional cardiology procedures were prospectively enrolled. Exclusion criteria were as follows: myocardial infarction (MI) diagnosed within the last 3 months, arrhythmia, renal insufficiency, or contraindications for MRI. Fifty patients underwent CMR 12–48 hours before PCI. Of these, 38 patients had successful CTO-PCI, of whom eight refused to undergo reinvestigation. Finally, 30 patients {6 females, 24 males; mean age (standard deviation [SD]), 57 ± 12 years}, who had undergone baseline CMR, successful CTO-PCI, and follow-up CMR at 6 ± 1 months post-PCI were included in this study. PCI failure was associated with an inability to pass the guidewire through the occlusion in nine patients, failure to perform balloon intervention in 2, and failure to dilate the lesion in one patient. Venous blood sampling was conducted to measure hematocrit immediately prior to CMR. Some of the patients completing follow-up scans have been briefly described previously (15).

CMR

A clinical 1.5T Siemens MAGNETOM Aera scanner (Siemens Healthcare, Erlangen, Germany) was used for CMR procedures before and 6 months after PCI. Steady-state free precession (SSFP) cine MR imaging was performed. Imaging parameters were 2.5/1.1 ms, 80° flip angle, and Generalized Auto-calibrating Partially Parallel Acquisition (GRAPPA) with an acceleration factor of 2. T1 time was measured using an ECG-gated modified Look-Locker Inversion Recovery (MOLLI) sequence acquired in the basal, mid-ventricular, and apical short-axes before and 15 minutes after administration of 0.2 mmol/kg gadopentetate dimeglumine (Magnevist; Bayer AG, Berlin, Germany). Pre-contrast MOLLI protocols were based on two inversions and a 5- and -3 sampling scheme with three additional heartbeats for recovery between inversions. The post-contrast MOLLI sequences used three inversions and a 4-3-2 sampling strategy with an additional heartbeat for recovery. A non-selective inversion pulse with single-shot SSFP readout was conducted during MOLLI sequences. Specific imaging parameters included repetition time (TR)/echo time (TE)/flip angle of 2.3 ms/1.1 ms/35°, 360-mm field of view, 8-mm slice thickness, 120-ms minimum

ECV Predicts the LV Functional Outcome

inversion time (TI), 80-ms TI increment, partial Fourier 7/8 reconstruction, and GRAPPA with a parallel acquisition factor of 2. Finally, LGE images were acquired 10 minutes post-injection of contrast agent using a breath-hold segmented phase-sensitive inversion recovery sequence (TR/TE/TI/flip angle/voxel size: 11 ms/3 ms/300 ms/25°/1.3 x 1.3 x 8 mm³). To ensure similar slice positioning, care was taken to align the most basal section of the short-axis stack to the level of the mitral annulus in the end diastole both for baseline and follow-up scans. Slice positions of T1 mapping were matched by copying the respective positions of the acquired cine images.

Coronary Angiography

Collateral circulation was graded using Rentrop classification (0 = no collateral flow; 1 = filling of side branches; 2 = partial filling of the epicardial segment of the

occluded vessel; and 3 = complete filling of the epicardial segment) (7) by an experienced cardiologist who was blinded to the clinical details and CMR results. To compare segmental differences, the collateral circulation was divided into poorly developed (grades 0–2) or well-developed (grade 3) collaterals.

Image Analysis

Images were analyzed using cvi⁴² software (Circle Cardiovascular Imaging Inc., Calgary, Canada). All images were independently analyzed by a single experienced radiologist, who was unaware of the clinical data and outcome of the patients. Intraobserver agreement for imaging parameters was determined by the same reviewer who reanalyzed the data with a time interval of more than 2 weeks. Interobserver agreement was assessed by a second reviewer. Segmental wall thickening (SWT) was

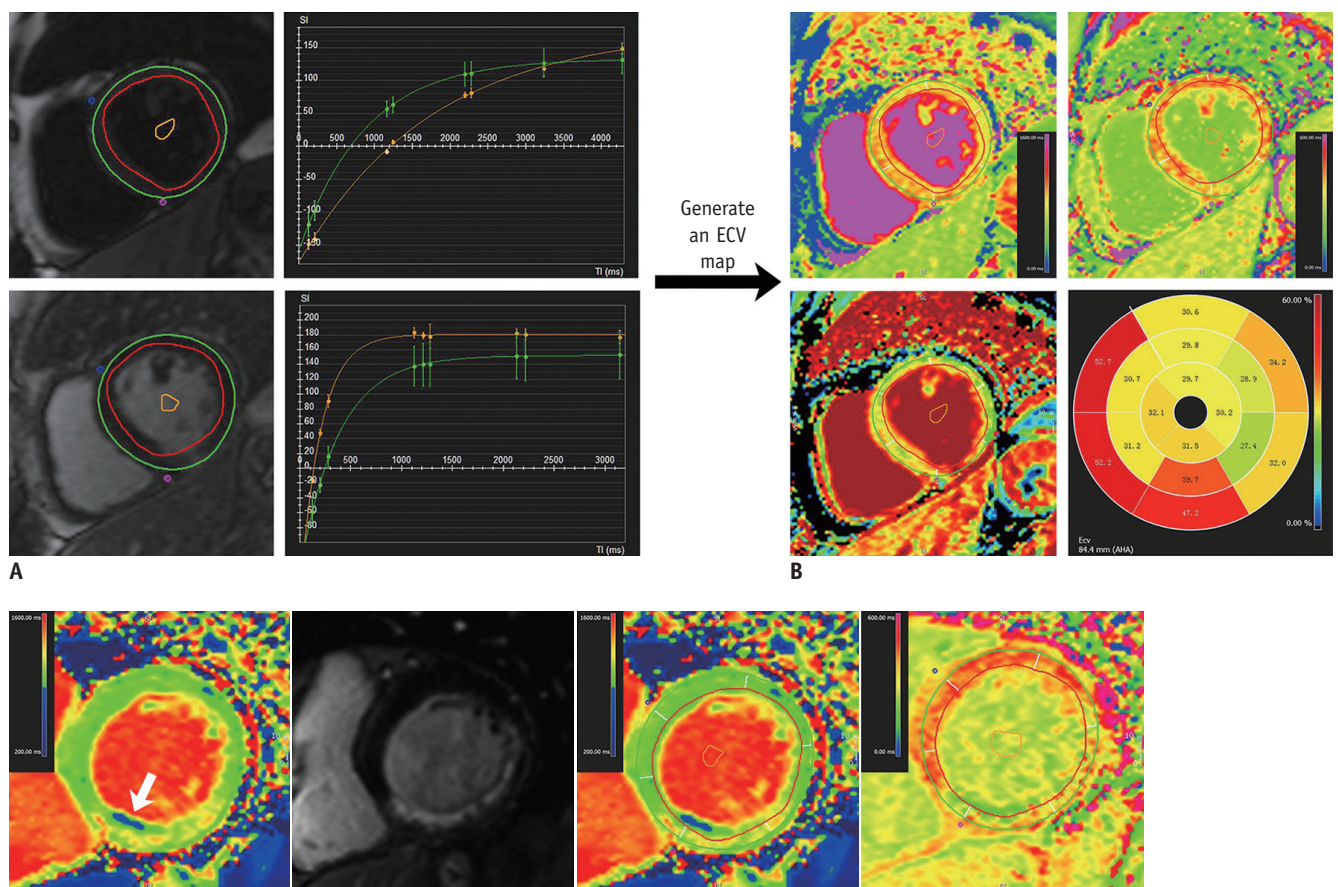


Fig. 1. Measurement of ECV based on AHA 16-segment model in patients with right coronary artery chronic total occlusion.

A. "T1 Calculation" module required endocardial and epicardial contours, segmentation points and blood-pool contour in all slices in both T1 maps. **B.** "Map Analysis" module generated ECV map and polar map when hematocrit was entered and long axis extent was defined. Note that AHA 2 and 3 segments were located at outflow tract. **C.** In another case with chronic fatty infiltration (arrow), contours were drawn avoiding zone with abnormal low native T1 times, and copied to matched post-contrast T1 map. AHA = American Heart Association, ECV = extracellular volume fraction

calculated by the formula: (end-systolic wall thickness - EDWT) / EDWT x 100%, where EDWT represents end-diastolic wall thickness. Manual correction was performed when the delineation of endo- and epi-myocardial outlines was inappropriate. Myocardial segments in the perfusion territory of a CTO vessel were then pre-selected if they were dysfunctional and successfully revascularized. SWT less than 45% indicated myocardial segment dysfunction (9). Assignment of myocardial segments to the perfusion territory of CTO vessels was based on the American Heart Association scientific statement (16).

For per-segment analysis, three markers at baseline, TEI, RIM, and ECV were evaluated. Contrast-enhanced regions were identified on LGE images by using a 5 SD threshold above the mean signal intensity of remote myocardium, and TEI was defined as the ratio of the enhanced area of each segment to the segmental area, which was graded as 0–25%, 26–50%, 51–75%, and 76–100% (17). RIM refers to the average wall thickness of the unenhanced area of a segment (18) using the following formula: (100 - hyperenhanced area) x EDWT / 100. Mean segmental ECV was measured from matched T1 maps before and after contrast at the basal, middle, and apical slices. An ECV map was generated when the endocardial and epicardial contours, segmentation points, and a blood-pool contour were present in all slices of T1 maps (Fig. 1). Myocardial ECV was calculated based on the following equation (11):

$$ECV (\%) = (R1_{\text{myocardium post}} - R1_{\text{myocardium pre}}) / (R1_{\text{blood post}} - R1_{\text{blood pre}}) \times (100 - \text{hematocrit}), \text{ where } R1 = 1 / T1.$$

Segmental functional recovery refers to an absolute increase in SWT (> 10%) compared with baseline (9).

For per-patient analysis, LGE volume, global ECV, and remote ECV were respectively calculated both at baseline and follow-up. Global ECV represented the mean ECV of entire myocardium averaged by the basal, middle, and apical slices, while remote ECV excluded the regions positive of LGE. Changes in ECV were defined as the ratio of ΔECV (ECV at follow-up minus ECV baseline) to the baseline ECV value. LV ejection fraction (LVEF) absolute changes exceeding 5% at follow-up were deemed significant (19, 20) and used as the reference standard for global functional recovery.

Statistical Analysis

Data were expressed as mean \pm SD or median and interquartile range as appropriate. Baseline and follow-up values of SWT were evaluated using paired Student's *t* test. Receive operating characteristic analyses were

performed to define the best cutoff value to discriminate between segments with and without functional recovery, based on the reference standard of an increase of > 10% in SWT. Differences in sensitivity and specificity were compared using McNemar's chi-squared tests. Differences in segmental values were evaluated using a mixed linear model to account for non-independence of segmental data within each patient. Continuous variables were correlated using Pearson's correlation coefficients. Stepwise logistic regression analysis was used to determine the independent predictors of regional and global functional recovery. Variables with a *p* value < 0.1 in the univariate linear regression were included in a multiple linear regression analysis to respectively investigate the determinants of EF

Table 1. Patient Baseline Characteristics

Age	57 \pm 12
Male	24 (80)
Body mass index (kg/m ²)	25.3 \pm 3.0
Heart rate	64 \pm 6
Follow up period (months)	6 (5–6.5)
Risk factors	
Hypertension	18 (60)
Diabetes mellitus	11 (37)
Hyperlipidemia	10 (33)
Smoking	14 (47)
Presenting symptom	
Stable angina	21 (70)
Unstable angina	6 (20)
Silent ischemia	3 (10)
Location of CTO lesion	
LAD	11 (37)
LCX	3 (10)
RCA	13 (43)
Two vessel CTO	3 (10)
Formation of collateral circulation	
Well-developed	12 (40)
Poorly-developed	18 (60)
Hematocrit (%)	40.9 \pm 4.2
CKMB (ng/mL)	11.1 \pm 2.3
CTnT (ng/mL)	0.008 (0.006–0.013)
NT-proBNP (pg/mL)	119.9 (66.8–207.9)
EF (%)	51 \pm 7
LGE volume (mL) (n = 16)	11.7 \pm 9.1
LGE size (cm ²) (n = 16)	2.5 \pm 1.5

Data presented as mean \pm standard deviation, n (%), or median (interquartile range). CKMB = creatine kinase-MB, CTnT = cardiac troponin T, CTO = chronic total occlusion, EF = ejection fraction, LAD = left anterior descending branch, LCX = left circumflex artery, LGE = late gadolinium enhancement, NT-proBNP = N-terminal pro-brain-type natriuretic peptide, RCA = right coronary artery

at follow-up and changes in EF, and collinearity diagnostics were conducted to observe and correct the multi-collinearity. Intraobserver and interobserver variabilities and agreements were respectively assessed using Bland-Altman analysis and intraclass correlation coefficient r_{IC} . SAS software 9.3 (SAS Institute Inc., Cary, NC, USA) and MedCalc version 13 (MedCalc software, Mariakerke, Belgium) were used for statistical analyses.

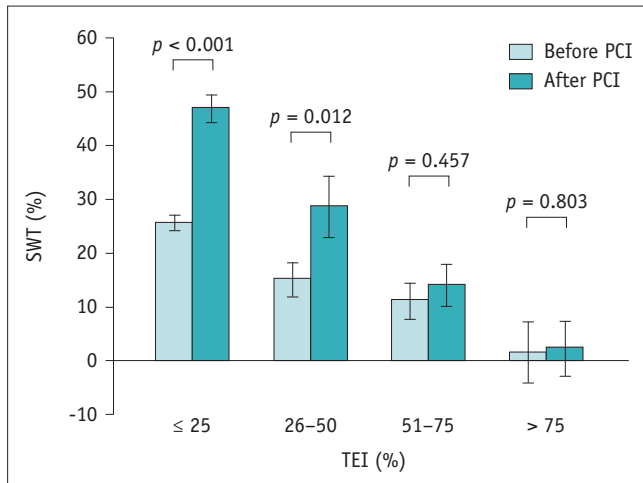


Fig. 2. Bar chart reveals inverse correlation between TEI and improvement in SWT. Bars and error bars represent means and 1 standard error of mean respectively. PCI = percutaneous coronary intervention, SWT = segmental wall thickening, TEI = transmural extent of infarction

Table 2. Intraobserver and Interobserver Variabilities in and Agreements for SWT and Imaging Biomarkers

Parameters	Intraobserver	Interobserver
SWT (%)		
SWT at baseline	-0.6 ± 5.3 ($r_{IC} = 0.93$)	0.5 ± 6.2 ($r_{IC} = 0.92$)
SWT at follow-up	-0.8 ± 5.9 ($r_{IC} = 0.92$)	0.3 ± 7.0 ($r_{IC} = 0.90$)
Improved SWT	-0.2 ± 4.4 ($r_{IC} = 0.95$)	-0.1 ± 4.6 ($r_{IC} = 0.94$)
ECV (%)	0.2 ± 2.8 ($r_{IC} = 0.97$)	-0.4 ± 3.0 ($r_{IC} = 0.97$)
TEI		
(transmurality, %)	-0.7 ± 6.3 ($r_{IC} = 0.95$)	-1.0 ± 7.2 ($r_{IC} = 0.93$)
RIM (mm)	-0.1 ± 0.9 ($r_{IC} = 0.93$)	0.3 ± 1.1 ($r_{IC} = 0.92$)

Data are presented as differences (intraclass correlation coefficient r_{IC}). ECV = extracellular volume fraction, RIM = unenhanced rim thickness, SWT = segmental wall thickening, TEI = transmural extent of infarction

Table 3. Predictive Performance of Baseline Markers in Segmental Function Recovery after Revascularization

Parameters	Cutoff Value	AUC (95% CI for AUC)	P	Sens. (%)	Spec. (%)	PPV (%)	NPV (%)
ECV	34.7%	0.86 (78, 92)	< 0.001	91 (67/74)	66 (34/52)	79 (67/85)	83 (34/41)
TEI	25%	0.75 (65, 83)	< 0.001	81 (60/74)	63 (33/52)	76 (60/79)	70 (33/47)
RIM	5.0 mm	0.73 (63, 82)	< 0.001	89 (66/74)	58 (30/52)	75 (66/88)	79 (30/38)

AUC = area under receiver operating characteristic curve, CI = confidence interval, NPV = negative predictive value, PPV = positive predictive value, sens. = sensitivity, spec. = specificity

RESULTS

Patient Characteristics

Patient demographics are shown in Table 1. Twelve patients presented well-developed collateral circulation on coronary angiography, and the remaining patients showed poorly developed collaterals. Six cases showed chronic fatty infiltration (Fig. 1C). In the 30 patients who completed follow-up scans, 177 segments were in the perfusion territory of the CTO, among which 126 were considered dysfunctional and enrolled for per-segment analysis.

Segmental Wall Motion

The baseline mean SWT of the dysfunctional segments was $20 \pm 14\%$, which increased to $36 \pm 25\%$ at 6 months ($p < 0.001$). In segments with $\leq 25\%$ ($n = 80$) TEI and 26–50% TEI ($n = 19$), the mean SWT increased significantly after revascularization ($26 \pm 11\%$ – $47 \pm 21\%$ and $15 \pm 12\%$ – $29 \pm 23\%$, $p < 0.001$ and $p = 0.012$, respectively). SWT showed an increasing trend in segments with 51–75% TEI ($n = 22$, $11 \pm 14\%$ – $14 \pm 16\%$, $p = 0.457$), and remained unchanged ($2 \pm 13\%$ – $2 \pm 11\%$, $p = 0.803$) in five segments with TEI > 75% (Fig. 2). The intra- and interobserver repeatabilities of SWT are depicted in Table 2.

Prediction of Segmental Functional Recovery and the Role of Collateral Circulation

The predictive value of the imaging markers is shown in Table 3. The 25% and 50% cutoff values of TEI had no impact on the predictive performance (area under receiver operating characteristic curve [AUC]: TEI₂₅ 0.75 vs. TEI₅₀ 0.71, $p = 0.328$). Segmental ECV predicted regional functional recovery better than TEI or RIM (all p values < 0.010) (Fig. 3). In the segments showing conflicting findings for the outcome obtained by TEI and/or RIM ($n = 36$), ECV was the best predictor of regional functional recovery with a diagnostic accuracy of 36% (13/36), compared with that of 8% for TEI (3/36, $p < 0.001$) and 17% for RIM (6/36, $p = 0.002$). Specifically, the sensitivity of ECV was greater than that of TEI (57% vs. 0%, $p = 0.031$),

whereas its specificity was superior to that of TEI (23% vs. 14%, $p = 0.003$) and RIM (23% vs. 0%, $p < 0.001$).

Intraclass correlation coefficients indicating intraobserver agreement for measurement of segmental ECV, TEI, and RIM were 0.97, 0.95, and 0.93, respectively. The corresponding interobserver agreement values for measurement of segmental ECV, TEI, and RIM were 0.97, 0.93, and 0.92, respectively (Table 2).

As for the influence of collateral circulation on wall motion, Table 4 demonstrated that well-developed collaterals were associated with a higher SWT at follow-

up, and a larger baseline SWT ($p = 0.077$) and SWT improvement for a strong trend ($p = 0.081$). Additionally, formation of collaterals correlated with TEI, and tended to relate to the segmental ECV ($p = 0.064$). However, the statistical significance of collateral circulation was not observed for prediction of segmental functional recovery both in univariate and multivariate logistic regression analysis, which revealed mean segmental ECV as the only independent predictors of regional functional outcome after PCI (odds ratio [OR] = 0.83, 95% confidence interval [CI]: 0.77–0.89; $p < 0.001$) (Table 5).

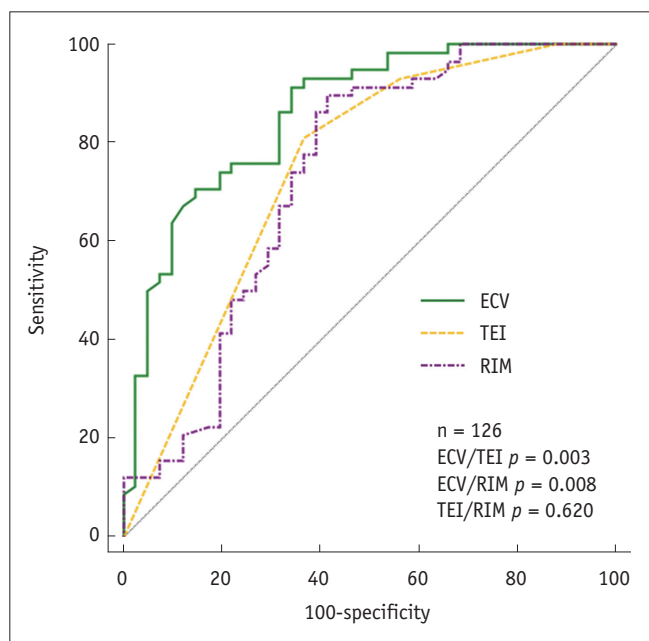


Fig. 3. ROC curves demonstrating diagnostic performance of baseline imaging markers in predicting segmental function recovery. RIM = unenhanced rim thickness, ROC = receive operating characteristic

Correlates of ECV with SWT

As illustrated in Figure 4, SWT at 6 months was significantly inversely correlated with the baseline segmental ECV according to both threshold-based ($p < 0.001$) and regression analysis ($r = -0.69$, $p < 0.001$).

Table 5. Predictors of Segmental FR in Logistic Univariate and Multivariate Regression Analysis

	OR	95% CI for OR	P
Univariate			
Location of CTO lesion	0.66	0.29–1.50	0.324
Collateral circulation	1.76	0.72–4.29	0.214
SWT at baseline	1.04	1.01–1.07	0.020
EDWT	1.23	0.98–1.55	0.070
TEI	0.28	0.16–0.50	< 0.001
RIM	1.41	1.19–1.67	< 0.001
Native T1 time	0.989	0.982–0.995	0.001
Post-contrast T1 time	1.02	1.01–1.03	< 0.001
ECV	0.83	0.77–0.89	< 0.001
Multivariate			
ECV	0.83	0.77–0.89	< 0.001

OR = odds ratio

Table 4. Comparison of Segmental Parameters between Poorly and Well-Developed Collateral Circulation

Parameters	Poorly-Developed (n = 86)	Well-Developed (n = 40)	P
Segment with FR/without FR	47/39	27/13	0.255
Location of CTO lesion (LAD/non-LAD territory)	43/43	29/11	0.161
EDWT (mm)	8.4 ± 1.9	8.9 ± 1.8	0.513
TEI	1 (1–3)	1 (1–1)	0.036*
RIM (mm)	6.4 ± 3.2	7.9 ± 2.2	0.114
Native T1 time (ms)	1060 ± 85	1031 ± 86	0.336
Post-contrast T1 time (ms)	388 ± 64	408 ± 80	0.469
ECV (%)	32.8 ± 9.7	27.9 ± 6.6	0.064 [†]
SWT at baseline (%)	18.2 ± 14.0	25.1 ± 11.3	0.077 [†]
SWT at follow up (%)	31.2 ± 24.6	47.4 ± 21.0	0.024*
SWT improvement (%)	13.3 ± 18.8	22.3 ± 20.2	0.081 [†]

* $p < 0.05$, [†] $p < 0.10$. EDWT = end-diastolic wall thickness, FR = functional recovery

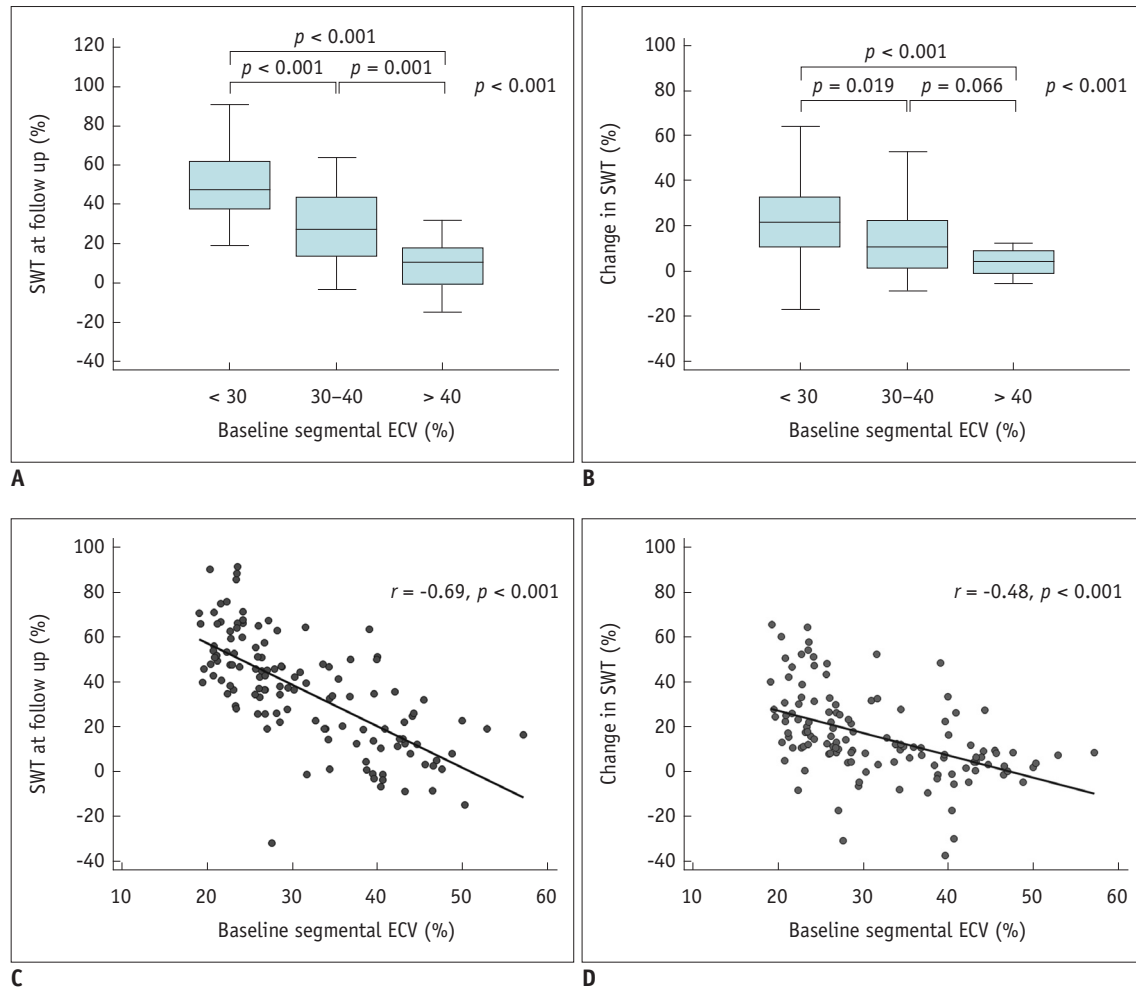


Fig. 4. Correlation between baseline segmental ECV, SWT at follow-up (A, C), and change in SWT from follow-up to baseline (B, D).

Likewise, changes in SWT from baseline to 6 months after revascularization correlated with segmental ECV ($p < 0.001$); however, there was an overlap in segments with 30–40% and > 40% ECV ($p = 0.066$). A moderate negative correlation between the segmental ECV and changes in SWT ($r = -0.48$, $p < 0.001$) was also found.

Prediction of Global Contractile Function and Functional Recovery

Revascularization significantly enhanced the mean LVEF in comparison with baseline ($54.5 \pm 8.5\%$ vs. $50.7 \pm 6.6\%$, $p < 0.001$). Seventeen patients (57%) demonstrated significant improvement in LVEF after revascularization (53.1 ± 3.6 – 60.3 ± 4.1 , $p < 0.001$), whereas the remaining 13 patients showed no significant improvement in EF. Univariable linear regression analysis demonstrated that collateral circulation was significantly associated with EF at follow-up ($r = 0.38$, $p = 0.049$). Moreover, global ECV, but not remote ECV, and

LGE volume on the patient level had a negative relationship with EF at follow-up. In multivariate regression analysis, global ECV ($\beta = -0.61$, $p < 0.001$) and cardiac troponin T (CTnT) ($\beta = -0.33$, $p = 0.026$) still showed a significant relationship, whereas collaterals and LGE volume did not. Among determinants of changes in EF, global ECV ($\beta = -0.57$, $p = 0.001$) and follow-up period ($\beta = 0.38$, $p = 0.022$) remained significant after adjusting for various parameters (Table 6).

According to the results of multivariate binary logistic regression analysis, the global baseline ECV differentiated between patients with significant EF improvement and without post-revascularization (OR, 0.38; 95% CI, 0.17–0.85; $p = 0.019$), independently of LGE volume, remote ECV, collateral circulation, follow-up period, as well as demographic and laboratory parameters. The AUC was 0.93 ($p < 0.001$) for global ECV with a cutoff value of 30.0 (sensitivity, 94%; specificity, 80%; positive predictive

Table 6. Predictors of EF at Follow-Up and Changes in EF by Regression Analysis

	EF at Follow Up				Change in EF			
	Univariate		Multivariate		Univariate		Multivariate	
	<i>r</i>	<i>P</i>	β	<i>P</i>	<i>r</i>	<i>P</i>	β	<i>P</i>
Age	-0.19	0.346			-0.03	0.879		
Sex	-0.29	0.149			-0.18	0.371		
Hypertension	-0.11	0.578			-0.20	0.317		
Diabetes	0.08	0.700			0.05	0.817		
Hyperlipidemia	0.24	0.233			0.38	0.052	0.13	0.508
Smoking	-0.22	0.278			-0.18	0.361		
Heart rate	0.37	0.055	0.24	0.080	0.03	0.902		
Presenting symptom	0.02	0.908			0.15	0.462		
CKMB	0.22	0.276			-0.01	0.959		
CTnT	-0.52	0.006	-0.33	0.026*	-0.27	0.175		
NT-proBNP	-0.40	0.038	0.13	0.504	-0.42	0.029	-0.25	0.130
CTO location	0.01	0.970			0.18	0.371		
Collateral circulation	0.38	0.049	0.09	0.524	0.18	0.375		
Follow up period	0.05	0.810			0.34	0.086	0.38	0.022*
Global ECV	-0.71	< 0.001	-0.61	< 0.001*	-0.55	0.003	-0.57	0.001*
Change in global ECV	0.23	0.256			0.20	0.313		
Remote ECV	-0.26	0.183			-0.25	0.201		
Change in remote ECV	0.19	0.352			0.19	0.346		
LGE volume	-0.62	0.001	-0.22	0.214	-0.42	0.03	0.04	0.866

**p* < 0.05

value, 89%; negative predictive value, 89%) (Fig. 5).

DISCUSSION

This study demonstrated that ECV can complement LGE as a better prognostic biomarker of regional and global functional outcome 6 months following revascularization in patients with CTO. We found that dysfunctional segments were likely to recover regional function if $ECV \leq 34.7$, $TEI \leq 25\%$, or $RIM \geq 5.0$ mm. Segmental ECV functioned as the only determinant of regional functional outcome independently of other imaging markers and collateral circulation. The global ECV at baseline per patient was tightly correlated with EF at follow-up and with changes in EF, and also identified the patients with significant EF improvement with a cutoff value of 30.0 that was independent of the LGE extent.

Transmural extent of infarction assessments obtained by CMR are regarded as a prognostic marker. In the present study, the decreased possibility of restoration of segmental function with increased TEI was consistent with the findings of previous studies (21-23). Although LGE is more sensitive than PET for nontransmural infarction, its accuracy is reduced in segments with intermediate TEI, showing

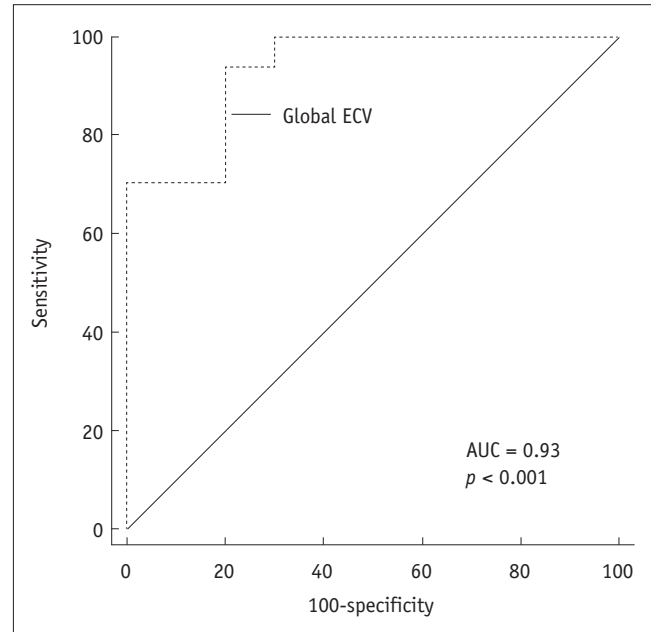


Fig. 5. ROC curves for prediction of significant improvement in ejection fraction based on global ECV at baseline. AUC = area under receiver operating characteristic curve

varying rates of functional restoration ranging from 10% to 60% (17, 20, 24, 25). From a histological point of view, the foci of preserved myocytes were found within myocardial

infarcts (26), whereas LGE failed to grade the severity of myocardial injury, partly accounting for the wide range of functional recovery potentials. To overcome the limitation, an accurate and reliable method to depict the severity of injury rather than just the volume of injury in dysfunctional myocardium is highly desirable.

Extracellular volume fraction provides a continuous measurement of extracellular space, and thus acts as a novel tool to interrogate the severity of myocardial injury. In our results, segmental ECV allowed for prediction of functional outcome. The more severe myocardial damage is, the larger the extracellular space and greater is the ECV, resulting in a decreased rate of functional recovery. Furthermore, a better performance of ECV was noted in comparison with TEI and RIM, which was also validated in models of acute MI (27). This may be attributable to the different imaging mechanisms among these baseline markers. LGE helps assess the amount of non-viable myocardium but does not take into account the severity of tissue damage within the infarcted myocardium, nor the epicardial unenhanced rim. RIM only considers the thickness of the unenhanced area; besides, its calculation process, which is dependent on TEI and wall thickness, would lessen its clinical applicability. Segmental ECV integrates both the degenerative change within the infarcted myocardium and epicardial unenhanced rim, thus providing a comprehensive evaluation of segmental characterization, as well as showing more relative importance as a determinant of functional recovery. Although the diagnostic accuracy of segmental ECV was relatively low in the segments showing conflicting findings with functional outcomes, the technique still showed favorable performance in predicting the prognosis, which further confirmed the value of ECV.

The presence of well-developed collateral circulation plays a protective role in the downstream myocardium assigned to CTO vessels. Our previous study showed, as it already has been demonstrated by Chen et al. (6), Choi et al. (7), and Zhang et al. (28), that well-developed collaterals were associated with a lower incidence of MI, lower transmural LGE and LGE volume, and reduced regional wall motion abnormality score. Studies to date have mainly focused on the relationship between collateral circulation and baseline CMR markers. In the present study, a positive relationship with regional wall motion at follow-up was also found. A latest publication has reported that the healing of myocardial injury, as defined by $\Delta T1$ from the acute to chronic stages, was closely related to the

microcirculation function (29). Therefore, we conjectured that a well-developed collateral circulation may give rise to a less damaged myocardial segment, as depicted by a lower segmental ECV ($p = 0.064$) in the present study, and a more efficient myocardial healing process, thus showing a smaller portion of degenerative and dysfunctional myocardium and a higher SWT at follow-up. Although the collaterals exerted no influence on predicting segmental functional recovery, our findings maintained that collateral circulation at angiography facilitates earlier assessment of regional systolic function after revascularization.

Changes in the LVEF after successful recanalization of CTO have been illustrated with mixed results. In our cohort, a small but significant improvement in EF ($54.5 \pm 8.5\%$ vs. $50.7 \pm 6.6\%$, $p < 0.001$) was noted after revascularization, which was in accordance with previously published results (4, 30, 31). Chadid et al. (5) reported that the increase in EF was confined to patients with baseline LVEF below the median of the cohort. In contrast, a significant decrease in end-diastolic volume with no significant improvement in EF has been reported (22, 25).

Various parameters, such as the extent of LGE, microvascular obstruction, global LV strain, etc. (32-34), have been recognized as predictors of global LV function after acute MI. To our knowledge, few studies have probed the predictors of global LV function after recanalization in CTO patients. Our findings have demonstrated that both the global ECV value and LGE volume were associated with EF at follow-up and changes in EF, while the latter gave way to CTnT and follow-up period in multivariate regression analysis. Moreover, global baseline ECV emerged as an independent predictor of significant EF improvement following revascularization (OR: 0.38; $p = 0.019$). This can be partly explained by the fact that the increase in ECV in the affected myocardium represents myocardial fibrosis, and is associated with impaired global function and adverse LV remodeling (27, 35, 36) and thus delayed or non-recovery of LV function at follow-up. Our study suggests that improved patient selection for revascularization can be achieved by CMR, which may help identify the patients most likely to experience beneficial LV systolic function improvement after CTO-PCI.

Our study has its limitations. First, the sample size in this study was small due to unsuccessful CTO-PCI procedures as well as the incidence of loss to follow-up. The unsuccessful PCI rate of 24% (12/50) in our study was acceptable compared with the previously published results (9, 22,

25). Further studies with more patients and long-term follow-up are warranted. Second, our results were derived from a specific population whose EF was normal or mildly impaired, and it remains unknown whether the conclusions could be applied to the patients with moderate to severe EF impairment. Third, the ECV changes with the increasing age, and the cutoff value in the present study may not suitable for other age groups. However, CTO patients have a narrower age range, mainly 55–75 years (37), which broadly agreed with the present study. Therefore, it is feasible to apply the current cutoff value to the other CTO cohort. Finally, sustained recanalization at follow-up was not confirmed angiographically in all the patients. However, the lack of symptoms and absence of a new LGE zone at follow-up can exclude graft occlusion or in-stent restenosis.

In conclusion, non-invasive assessment of ECV provides incremental value in comparison with conventional CMR measures and remains the only predictor of functional outcome both at the segmental and global levels in patients with CTO. The clinical relevance of ECV potentially allows for improved early prognostication and resource allocation to patients who are more likely to benefit from CTO-PCI.

Conflicts of Interest

The authors have no financial conflicts of interest.

Acknowledgments

The authors thank Xue Juan Jin for providing the statistical advice for this manuscript.

ORCID

Mengsu Zeng

<https://orcid.org/0000-0001-6054-0824>

Yinyin Chen

<https://orcid.org/0000-0002-1192-671X>

REFERENCES

1. Brilakis ES, Karpaliotis D, Vo MN, Garcia S, Michalis L, Alaswad K, et al. Advances in the management of coronary chronic total occlusions. *J Cardiovasc Transl Res* 2014;7:426-436
2. Christofferson RD, Lehmann KG, Martin GV, Every N, Caldwell JH, Kapadia SR. Effect of chronic total coronary occlusion on treatment strategy. *Am J Cardiol* 2005;95:1088-1091
3. Christakopoulos GE, Christopoulos G, Carlino M, Jeroudi OM, Roesle M, Rangan BV, et al. Meta-analysis of clinical outcomes of patients who underwent percutaneous coronary interventions for chronic total occlusions. *Am J Cardiol* 2015;115:1367-1375
4. Pujadas S, Martin V, Rosselló X, Carreras F, Barros A, Leta R, et al. Improvement of myocardial function and perfusion after successful percutaneous revascularization in patients with chronic total coronary occlusion. *Int J Cardiol* 2013;169:147-152
5. Chadid P, Markovic S, Bernhardt P, Hombach V, Rottbauer W, Wöhrle J. Improvement of regional and global left ventricular function in magnetic resonance imaging after recanalization of true coronary chronic total occlusions. *Cardiovasc Revasc Med* 2015;16:228-232
6. Chen YY, Zhang WG, Yang S, Yun H, Deng SM, Fu CX, et al. Extracellular volume fraction in coronary chronic total occlusion patients. *Int J Cardiovasc Imaging* 2015;31:1211-1211
7. Choi JH, Chang SA, Choi JO, Song YB, Hahn JY, Choi SH, et al. Frequency of myocardial infarction and its relationship to angiographic collateral flow in territories supplied by chronically occluded coronary arteries. *Circulation* 2013;127:703-709
8. Romero J, Xue X, Gonzalez W, Garcia MJ. CMR imaging assessing viability in patients with chronic ventricular dysfunction due to coronary artery disease: a meta-analysis of prospective trials. *JACC Cardiovasc Imaging* 2012;5:494-508
9. Kirschbaum SW, Rossi A, Boersma E, Springeling T, van de Ent M, Krestin GP, et al. Combining magnetic resonance viability variables better predicts improvement of myocardial function prior to percutaneous coronary intervention. *Int J Cardiol* 2012;159:192-197
10. Knuesel PR, Nanz D, Wyss C, Buechi M, Kaufmann PA, von Schulthess GK, et al. Characterization of dysfunctional myocardium by positron emission tomography and magnetic resonance: relation to functional outcome after revascularization. *Circulation* 2003;108:1095-1100
11. Arheden H, Saeed M, Higgins CB, Gao DW, Bremerich J, Wyttenbach R, et al. Measurement of the distribution volume of gadopentetate dimeglumine at echo-planar MR imaging to quantify myocardial infarction: comparison with 99mTc-DTPA autoradiography in rats. *Radiology* 1999;211:698-708
12. Ugander M, Oki AJ, Hsu LY, Kellman P, Greiser A, Aletras AH, et al. Extracellular volume imaging by magnetic resonance imaging provides insights into overt and sub-clinical myocardial pathology. *Eur Heart J* 2012;33:1268-1278
13. Bauner KU, Biffar A, Theisen D, Greiser A, Zech CJ, Nguyen ET, et al. Extracellular volume fractions in chronic myocardial infarction. *Invest Radiol* 2012;47:538-545
14. Kirschbaum SW, Rossi A, van Domburg RT, Gruszczynska K, Krestin GP, Serruys PW, et al. Contractile reserve in segments with nontransmural infarction in chronic dysfunctional myocardium using low-dose dobutamine CMR. *JACC Cardiovasc Imaging* 2010;3:614-622
15. Chen YY, Ren DY, Zeng MS, Yang S, Yun H, Fu CX, et al. Myocardial extracellular volume fraction measurement in chronic total coronary occlusion: association with myocardial injury, angiographic collateral flow, and functional recovery. *J*

- Magn Reson Imaging* 2016;44:972-982
16. Cerqueira MD, Weissman NJ, Dilsizian V, Jacobs AK, Kaul S, Laskey WK, et al.; American Heart Association Writing Group on Myocardial Segmentation and Registration for Cardiac Imaging. Standardized myocardial segmentation and nomenclature for tomographic imaging of the heart. A statement for healthcare professionals from the Cardiac Imaging Committee of the Council on Clinical Cardiology of the American Heart Association. *Int J Cardiovasc Imaging* 2002;18:539-542
 17. Kim RJ, Wu E, Rafael A, Chen EL, Parker MA, Simonetti O, et al. The use of contrast-enhanced magnetic resonance imaging to identify reversible myocardial dysfunction. *N Engl J Med* 2000;343:1445-1453
 18. Rassaf T, Nolte J, Heussen N, Krombach GA, Günther RW, Kelm M, et al. Quantitation of the thickness of the non-enhanced myocardial rim predicts recovery of territorial myocardial function in chronic ischemic heart disease: a cardiac magnetic resonance imaging study. *Clin Res Cardiol* 2010;99:293-300
 19. Glaveckaite S, Valeviciene N, Palionis D, Puronaite R, Serpytis P, Laucevicius A. Prediction of long-term segmental and global functional recovery of hibernating myocardium after revascularisation based on low dose dobutamine and late gadolinium enhancement cardiovascular magnetic resonance. *J Cardiovasc Magn Reson* 2014;16:83
 20. Glaveckaite S, Valeviciene N, Palionis D, Skorniakov V, Celutkienė J, Tamosiunas A, et al. Value of scar imaging and inotropic reserve combination for the prediction of segmental and global left ventricular functional recovery after revascularisation. *J Cardiovasc Magn Reson* 2011;13:35
 21. Krittayaphong R, Laksanabunsong P, Maneesai A, Saiviroonporn P, Udompunturak S, Chaithiraphan V. Comparison of cardiovascular magnetic resonance of late gadolinium enhancement and diastolic wall thickness to predict recovery of left ventricular function after coronary artery bypass surgery. *J Cardiovasc Magn Reson* 2008;10:41
 22. Kirschbaum SW, Baks T, van den Ent M, Sianos G, Krestin GP, Serruys PW, et al. Evaluation of left ventricular function three years after percutaneous recanalization of chronic total coronary occlusions. *Am J Cardiol* 2008;101:179-185
 23. Bondarenko O, Beek AM, Twisk JW, Visser CA, van Rossum AC. Time course of functional recovery after revascularization of hibernating myocardium: a contrast-enhanced cardiovascular magnetic resonance study. *Eur Heart J* 2008;29:2000-2005
 24. Pegg TJ, Selvanayagam JB, Jennifer J, Francis JM, Karamitsos TD, Dall'Armellina E, et al. Prediction of global left ventricular functional recovery in patients with heart failure undergoing surgical revascularisation, based on late gadolinium enhancement cardiovascular magnetic resonance. *J Cardiovasc Magn Reson* 2010;12:56
 25. Baks T, van Geuns RJ, Duncker DJ, Cademartiri F, Mollet NR, Krestin GP, et al. Prediction of left ventricular function after drug-eluting stent implantation for chronic total coronary occlusions. *J Am Coll Cardiol* 2006;47:721-725
 26. Fishbein MC, Maclean D, Maroko PR. The histopathologic evolution of myocardial infarction. *Chest* 1978;73:843-849
 27. Kidambi A, Motwani M, Uddin A, Ripley DP, McDiarmid AK, Swoboda PP, et al. Myocardial extracellular volume estimation by CMR predicts functional recovery following acute MI. *JACC Cardiovasc Imaging* 2017;10:989-999
 28. Zhang J, Li Y, Li M, Pan J, Lu Z. Collateral vessel opacification with CT in patients with coronary total occlusion and its relationship with downstream myocardial infarction. *Radiology* 2014;271:703-710
 29. Liu D, Borlotti A, Viliani D, Jerosch-Herold M, Alkhalil M, De Maria GL, et al. CMR native T1 mapping allows differentiation of reversible versus irreversible myocardial damage in ST-segment-elevation myocardial infarction: an OxAMI Study (Oxford acute myocardial infarction). *Circ Cardiovasc Imaging* 2017;10. pii: e005986
 30. Bucciarelli-Ducci C, Auger D, Di Mario C, Locca D, Petryka J, O'Hanlon R, et al. CMR guidance for recanalization of coronary chronic total occlusion. *JACC Cardiovasc Imaging* 2016;9:547-556
 31. Nakachi T, Kato S, Kirigaya H, Iinuma N, Fukui K, Saito N, et al. Prediction of functional recovery after percutaneous coronary revascularization for chronic total occlusion using late gadolinium enhanced magnetic resonance imaging. *J Cardiol* 2017;69:836-842
 32. Altiok E, Tiemann S, Becker M, Koos R, Zwicker C, Schroeder J, et al. Myocardial deformation imaging by two-dimensional speckle-tracking echocardiography for prediction of global and segmental functional changes after acute myocardial infarction: a comparison with late gadolinium enhancement cardiac magnetic resonance. *J Am Soc Echocardiogr* 2014;27:249-257
 33. Carrick D, Haig C, Rauhalammi S, Ahmed N, Mordi I, McEntegart M, et al. Prognostic significance of infarct core pathology revealed by quantitative non-contrast in comparison with contrast cardiac magnetic resonance imaging in reperfused ST-elevation myocardial infarction survivors. *Eur Heart J* 2016;37:1044-1059
 34. Mollema SA, Delgado V, Bertini M, Antoni ML, Boersma E, Holman ER, et al. Viability assessment with global left ventricular longitudinal strain predicts recovery of left ventricular function after acute myocardial infarction. *Circ Cardiovasc Imaging* 2010;3:15-23
 35. Wong TC, Piehler K, Meier CG, Testa SM, Klock AM, Aneizi AA, et al. Association between extracellular matrix expansion quantified by cardiovascular magnetic resonance and short-term mortality. *Circulation* 2012;126:1206-1216
 36. Bulluck H, Rosmini S, Abdel-Gadir A, White SK, Bhuvana AN, Treibel TA, et al. Automated extracellular volume fraction mapping provides insights into the pathophysiology of left ventricular remodeling post-reperfused ST-elevation myocardial infarction. *J Am Heart Assoc* 2016;5. pii: e003555
 37. Fefer P, Knudtson ML, Cheema AN, Galbraith PD, Osherov AB, Yalonetsky S, et al. Current perspectives on coronary chronic total occlusions: the Canadian multicenter chronic total occlusions registry. *J Am Coll Cardiol* 2012;59:991-997